



Accuracy and Efficiency Analysis of the Beam Elements for Nonlinear Large Deformation

Zhen Wang¹ · Changle Xiang¹ · Hui Liu¹ · Ming Liu^{1,2}

Received: 15 April 2022 / Revised: 12 May 2022 / Accepted: 18 May 2022 / Published online: 20 June 2022
© Krishtel eMaging Solutions Private Limited 2022

Abstract

Purpose The purpose of this paper is to study that which beam element should be adopted to achieve the required high accuracy and efficiency in different projects. Three kinds of beam elements commonly used to analyze the nonlinear dynamics of flexible multibody systems are compared and analyzed, which are fully parameterized beam and gradient-deficient beam elements based on the absolute nodal coordinate formulation, and geometrically exact beam element, respectively.

Methods The governing equations are established based on the fully parameterized beam element, the gradient-deficient beam element and the geometrically exact beam element, and the generalized- α implicit time stepping algorithm is used to study the dynamic responses of system.

Results and Conclusion In this study, the solution accuracy and efficiency of the three kinds of element are analyzed in both statics and dynamics in detail and compared with each other. It is found that the geometrically exact beam element is superior to other two elements when the discretized element is subjected to axial deformation and torsion. Both gradient-deficient beam element and geometrically exact beam element show the high accuracy and efficiency when the element is bent. Moreover, the Young's modulus and time step have a great effect on displacement responses when the beam element is in dynamic state. All the results should be helpful for selection of a high-precision calculation method in engineering applications.

Keywords Fully parameterized beam element · Gradient-deficient beam element · Geometrically exact beam element · Accuracy · Nonlinear large deformation

Mathematics Subject Classification 70E55 · 74H45

Introduction

The investigation of the nonlinear coupling phenomenon in nonlinear dynamics is of great significance for a broad range of applications, including aerospace, robot and vehicle engineering. Due to the larger elastic deformation of flexible components, the high accuracy analysis is difficult to achieve using either the traditional multi-rigid-body system dynamics or flexible multi-body dynamics with small deformation. Therefore, the flexible multi-body dynamics model with large displacements and rotations is widely used in nonlinear

dynamics for its high calculation accuracy and efficiency [1–4]. Two commonly used methods are the absolute nodal coordinate formulation (ANCF) and the geometrically exact formulation (GEF).

Shabana [5] first proposed the ANCF method and further established a one-dimensional beam element model, which was called as the milestone in the development of flexible multi-body system dynamics [6, 7]. Such method was first applied to study the dynamics of flexible systems with large deformation by Escalona et al. [8]. Based on the ANCF method, a three-dimensional beam element [9, 10] and a planar beam element of gradient-deficient ANCF [11] were proposed, respectively. Gerstmayr et al. [12] extended the planar beam element of gradient-deficient ANCF to the spatial beam element of gradient-deficient ANCF. Subsequently, Schwarze et al. [13] proposed a reduced integration solid shell finite element. To investigate the thermoelastic effect on the deployment of space

✉ Ming Liu
liuming05.03@163.com

¹ School of Mechanical Engineering, Beijing Institute of Technology, Beijing 100081, China

² Institute of Advanced Structure Technology, Beijing Institute of Technology, Beijing 100081, China

structure, Wu et al. [14] proposed a new approach based on flexible multibody system. Sapanen and Mikkola [15] presented an accurately elastic force model to avoid the Poisson locking. Omar et al. [16] established a simplified model of leaf spring with the ANCF method. Liu et al. [17–19] proposed a new hybrid-coordinate formulation which was suitable for dealing with the flexible multibody systems with large deformation. Tian et al. [20–22] studied the dynamic modeling and analyzed the planar flexible multi-body systems with clearance and lubricated revolute joints. To model composite laminated plates accurately, Liu et al. [23] proposed a new type of composite laminated plate element of ANCF and derived the efficient formulations to evaluate both the elastic force and the Jacobian.

The other commonly used method was GEF theory, which was first proposed by Reissner [24]. Simo and Vu-Quoc [25] further improved the GEF theory by developing the implicit time stepping algorithm, the exact linearization of the algorithm and associated configuration update. In the field of study for limitation of invariance to rigid-body rotations, Crisfield et al. [26] proposed a new method for the two-node element by obtaining the relative rotation matrix and interpolating the rotation vector. Huang et al. [27] demonstrated that the obtained approximation is invariant under the superposed rigid body motions, and the objectivity of the continuum model is preserved.

From the above researches, it can be found that both the ANCF method and the GEF theory developed rapidly and widely used. To analyze the difference between the two theories, Romero [28] studied and compared the two methods in statics, they proposed that the ANCF theory should be considered for the codes that do not work with rotation variables, and when the concentrated moments and imposed rotations are needed to be sustained by the structural models, the GEF theory is suitable because these features cannot be achieved by the ANCF element. Subsequently, Bauchau et al. [29] performed a comparative analysis of both the computational accuracy and efficiency of the two methods on the two-dimensional plane. However, only some static response in two-dimensional plane are concerned, the systematic study on statics and dynamics which is much closer to the practical engineering have not been studied yet, especially the responses of the three-dimensional model.

Motivated by the aim mentioned above, the governing equations are established based on the ANCF fully parameterized beam element, the ANCF gradient-deficient beam element and the GEF beam element. Both the static and dynamic responses of the three-dimensional flexible multibody system with large deformation are simulated in detail, the characteristics of each element type for analyzing the nonlinear dynamics of flexible multibody systems are provided. Based on the results, the appropriate choice of

formulation for high calculation accuracy and efficiency in different applications is also given.

Theoretical Model of the Beam Element and Computational Strategy

ANCF Fully Parameterized Beam Element

The schematic of the three-dimensional fully parameterized beam element with two nodes is shown in Fig. 1, which is described by the absolute node coordinates.

The position vector of any point on the element can be expressed as [5, 6]

$$r = \bar{e}\bar{S}(\xi, \eta, \zeta) \tag{1}$$

where $\xi = x/l, \eta = y/l, \zeta = z/l, x, y, z$ are the local coordinates of the element, respectively, l is the length of the element. Generalized coordinates of the element can be expressed as

$$\bar{e} = [r_i \ r_{i,x} \ r_{i,y} \ r_{i,z} \ r_j \ r_{j,x} \ r_{j,y} \ r_{j,z}] \tag{2}$$

where $r_{i,x}, r_{i,y}, r_{i,z}$ represent the partial derivative vector of the position vector r along ξ, η, ζ direction, respectively, that is, $r_{i,x} = \partial r / \partial \xi, r_{i,y} = \partial r / \partial \eta, r_{i,z} = \partial r / \partial \zeta$. It can be found from Eq. (2) that there is one position vector and three slope vectors are defined on one node. The shape function of the beam element can be expressed as

$$\bar{S} = [S_1 \ S_2 \ S_3 \ S_4 \ S_5 \ S_6 \ S_7 \ S_8]^T \tag{3}$$

where $S_1 = 1 - 3\xi^2 + 2\xi^3, S_2 = l(\xi - 2\xi^2 + \xi^3), S_3 = l(\eta - \xi\eta), S_4 = l(\zeta - \xi\zeta), S_5 = 3\xi^2 - 2\xi^3, S_6 = l(-\xi^2 + \xi^3), S_7 = l\xi\eta, S_8 = l\xi\zeta$.

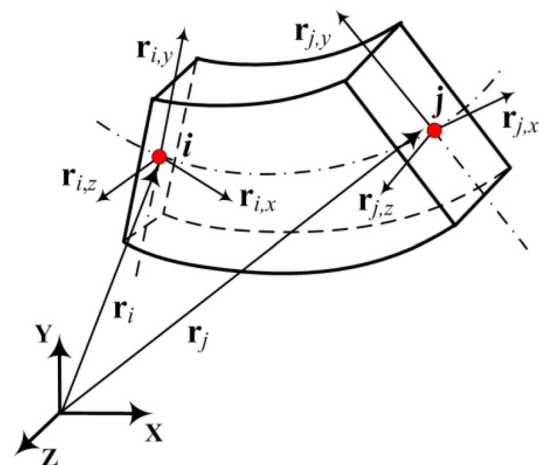


Fig. 1 The three-dimensional fully parameterized beam element

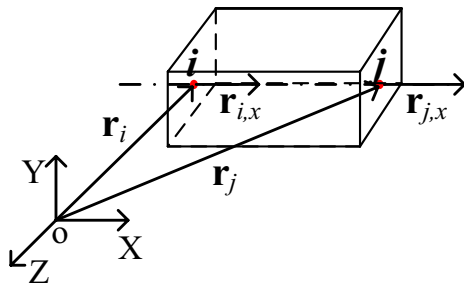


Fig. 2 The gradient-deficient beam element

In addition, it can be obtained by reference [5, 9] for more details on the ANCF fully parameterized beam element.

ANCF Gradient-Deficient Beam Element

The schematic of the ANCF gradient-deficient beam element described by absolute node coordinates is shown in Fig. 2.

Generalized coordinates of the element can be expressed as [30]

$$\bar{e} = [r_i \ r_{i,x} \ r_j \ r_{j,x}] \tag{4}$$

Both nodes include one position vector r and its partial derivative vector along ξ direction. The position vector of any point on the centerline can be expressed as

$$r(\xi) = \bar{e}\bar{S}(\xi) \tag{5}$$

The shape function of beam elements is expressed as

$$\bar{S} = [S_1 \ S_2 \ S_3 \ S_4]^T \tag{6}$$

where $S_1 = 1 - 3\xi^2 + 2\xi^3$, $S_2 = l(\xi - 2\xi^2 + \xi^3)$, $S_3 = 3\xi^2 - 2\xi^3$, and $S_4 = l(-\xi^2 + \xi^3)$.

In addition, it can be obtained by reference [30] for more details on the ANCF gradient-deficient beam element.

Three-Dimensional GEF Beam Element

Figure 3 shows the configurations of the three-dimensional beam element, which are described by three reference basis vectors denoted by k_1, k_2, k_3 and three body basis vectors denoted by $\lambda_1, \lambda_2, \lambda_3$.

The position vectors of the point before and after deformation are assumed as $x_0 = (x_0, y_0, z_0)^T$ and $x = (x, y, z)^T$, respectively. From the geometric relationship, the position vector can be derived as [8]

$$\begin{cases} x_0 = (x_0, y_0, z_0)^T = r_0 + y_0\lambda_1^0 + z_0\lambda_2^0 \\ x = (x, y, z)^T = r + y_0\lambda_1 + z_0\lambda_2 \end{cases} \tag{7}$$

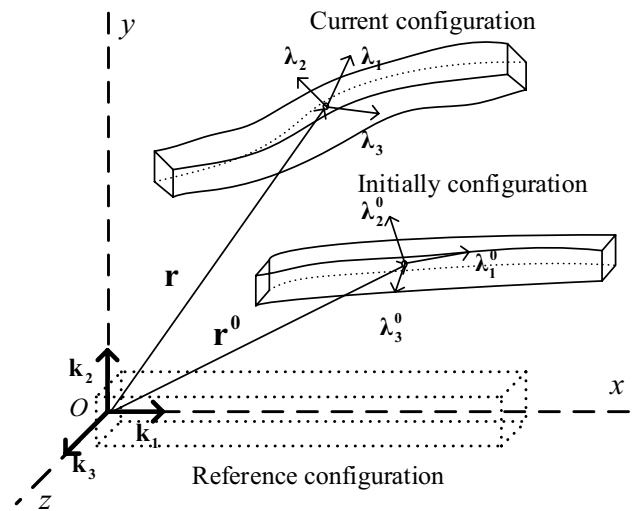


Fig. 3 Configurations of three-dimensional beam element

where r_0 and r are functions of x_0 , respectively. The expression of the deformation gradient tensor can be written as [31]

$$F = \frac{dx}{dx_0} = [r' + y_0\lambda_1' + z_0\lambda_2' \ \lambda_1 \ \lambda_2] \tag{8}$$

where represents the derivative along x direction.

To obtain the six objective strain metrics of the spatial GEF beam element, the translational strain vector γ and rotational strain vector κ are introduced as the following [32].

$$\gamma = \begin{Bmatrix} \varepsilon \\ \gamma_1 \\ \gamma_2 \end{Bmatrix} = R^T r' - \gamma_0, \kappa = \begin{bmatrix} 0 & -\kappa_3 & \kappa_2 \\ \kappa_3 & 0 & -\kappa_1 \\ -\kappa_2 & \kappa_1 & 0 \end{bmatrix} = R^T R - \kappa_0 \tag{9}$$

where R is the functions of x_0 , ε is the axial strain, γ_1 and γ_2 are shear strains of the beam element at the current reference frame $(\lambda_1, \lambda_2, \lambda_3)$. κ_1 is the torsional strains, κ_2 and κ_3 are the bending strains of the beam element at the current reference frame $(\lambda_1, \lambda_2, \lambda_3)$. κ_0 and γ_0 denote the curvature and the strain vector of the beam element at the initial configuration, respectively.

In addition, it can be obtained by reference [24, 25] for more details on the three-dimensional GEF beam element.

Computational Strategy

The assembly of both ANCF fully parameterized beam element and geometrically exact beam element can be carried out is similar to the traditional finite element method. The nodal coordinate on the finite element can be easily transformed into the generalized coordinate on the flexible multibody system. Then the final dynamic equations of the

constrained rigid-flexible multibody system [33, 34] can be expressed as:

$$\begin{cases} M\ddot{q} + F(q) + \Phi_q^T \lambda = Q(q, \dot{q}) \\ \Phi(q, t) = 0 \end{cases} \quad (10)$$

where M, q, F, Q, Φ, Φ_q , and λ denote the total mass matrix, the generalized coordinate vectors, the elastic force, the generalized external force vector, the system constraint equation, Jacobi matrix for generalized coordinates and the Lagrange multiplier vector, respectively.

Since the step limitation can be induced by the conditional convergence characteristics of the explicit integration algorithm and the implicit integral algorithm is always used to analyze such dynamic equations of the system, the transformation of the dynamic equations is required. The generalized-a implicit integral algorithm proposed by Arnold and Brüls [35] is applied here, during which the equations are discretized into algebraic equations by the finite difference method. The iterative equations can be expressed as

$$\begin{cases} M\ddot{q}_{n+1} + F(q_{n+1}) + \Phi_q^T \lambda_{n+1} - Q(q_{n+1}, \dot{q}_{n+1}) = 0 \\ \Phi(q_{n+1}, t_{n+1}) = 0 \end{cases} \quad (11)$$

where the subscript $n + 1$ represents the value of the variable at $n + 1$ step during the iteration. Tian et al. [36] and Liu et al. [37] reported that the superiority of the generalized-a implicit integral algorithm was exhibited in dealing with the dynamics of the flexible multibody system with clearance joints.

Results and Discussion

Static Response of the Beam Element

To investigate the accuracy and efficiency of the ANCF fully parameterized beam element, the ANCF gradient-deficient beam element and the GEF beam element, A representative numerical example of three-dimensional cantilever beam is adopted. The theoretical model is shown in Fig. 4. Because the cross-sectional deformation of beam is not involved

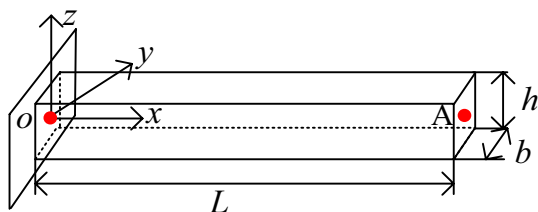


Fig. 4 Theoretical model of the cantilever beam

in the ANCF gradient-deficient beam element, only the displacement response of point A is studied, which is the geometric center of the free end section. In addition, the static responses calculated by the ABAQUS finite element software are regarded as the exact solutions, and the cantilever beam is divided into ten B32 elements. The geometric and material parameters of the cantilever beam are listed in Table 1.

For the axial deformation of the cantilever beam including axial tension and compression, a concentrated load F is applied on the point A along x direction. The displacements of point A calculated by different elements are listed in Table 2, in which Poisson’s ratio $\lambda=0.3$ and concentrated force of 1 kN, 10 kN, $- 1$ kN and $- 10$ kN are adopted. It can be found from Table 2 that the result calculated by GEF beam element has a good agreement with the exact solution no matter the beam is in tension or compression state, while the results based on both ANCF fully parameterized beam element and ANCF gradient-deficient beam element are smaller than the exact solution.

Due to the three-dimensional constitutive relation applied in ANCF fully parameterized beam element, the plane cross-section assumption is not applicable in the three-dimensional model and part of the energy provided by the external force is transformed into the deformation of the cross section, which leads to the smaller results of the ANCF fully parameterized beam element. The large-strain assumption is the factor that induces the smaller value of ANCF gradient-deficient beam element. The computational efficiency of the ANCF fully parameterized beam element is lower than that of the GEF beam element due to the longer time of calculating elastic force by the triple integral. Besides, the computational efficiency of the ANCF fully parameterized beam element is also lower than that of the ANCF gradient-deficient beam element due to the less degree of freedom of the ANCF gradient-deficient beam element. As a result, both the high calculation accuracy and efficiency can be achieved by the GEF beam element in the axial deformation of the cantilever beam.

For the plane bending deformation of the cantilever beam, the concentrated load along z direction is applied on the point A. The results are listed in Table 3, in which the cases with two values of λ are included to study the effect of Poisson’s ratio. The displacements of point A along x and z direction are denoted by u and w , respectively. Table 3 shows

Table 1 Geometric and material parameters of the cantilever beam

Young’s modulus E (Pa)	Density ρ (kg/m^3)	Width b (m)	Height h (m)	Beam length L (m)
7.2×10^{10}	2.7×10^3	0.01	0.01	1

that the result calculated by ANCF fully parameterized beam element becomes more accurate when the effect of Poisson’s blocking is removed by reducing λ from 0.3 to 0. Because the cross-sectional deformation of beam can be calculated by the precise geometric nonlinear relation in GEF beam element and that is not involved in the ANCF gradient-deficient beam element, the results based on the ANCF gradient-deficient beam element and the GEF beam element are not affected by the Poisson’s ratio. In comparison, the results obtained by both ANCF gradient-deficient beam element and GEF beam element are closer to the exact results than that of ANCF fully parameterized beam element.

For the bending deformation in three-dimension case, two concentrated loads of -50 N are applied simultaneously along y direction and z direction on point A. The results are provided in Table 4, in which the cases with two values of λ are adopted. Apparently, the results based on both the ANCF gradient-deficient beam element and the GEF beam element are in good agreement with the exact solutions in three directions, but the results based on the ANCF fully

parameterized beam element are relatively poor, especially when λ is 0.3.

The pure bending deformation of the cantilever beam is also studied by applying the moment M on point A around the z -axis. The angle of rotation α of the free end in this case can be expressed as [38]

$$\alpha = \frac{ML}{EI} \tag{12}$$

where M , EI , L denote the applied moment, flexural rigidity and beam length. Equation (12) shows that the angle of rotation increases with the increasing moment, it can be found that 360° angle of rotation can be obtained when M is $2\pi EI/L$, which is the typical nonlinear large deformation and can be regarded as the exact solution in the case of bending deformation of the cantilever beam.

To compare the high calculation accuracy and convergence rate, the beam is divided into 10, 20 and 30 elements, the results based on the above three elements are shown in Table 5. Table 5 shows that the number of convergence

Table 2 Displacements of point A when the cantilever beam is in axial deformation state

F (kN)	Displacement (mm)			
	ABAQUS	ANCF- full	ANCF-deficient	GEF
1	1.3889×10^{-1}	1.3661×10^{-1}	1.3722×10^{-1}	1.3889×10^{-1}
10	1.3889	1.3636	1.3697	1.3889
- 1	$- 1.3889 \times 10^{-1}$	$- 1.3664 \times 10^{-1}$	$- 1.3725 \times 10^{-1}$	$- 1.3889 \times 10^{-1}$
- 10	- 1.3889	- 1.3664	- 1.3725	- 1.3889

Table 3 Displacements of point A when the cantilever beam is in plane bending state

F (N)	Poisson’s ratio	Direction	Displacement (m)			
			ABAQUS	ANCF-full	ANCF- deficient	GEF
- 10	0	u	$- 1.8354 \times 10^{-3}$	$- 1.8316 \times 10^{-3}$	$- 1.8420 \times 10^{-3}$	$- 1.8422 \times 10^{-3}$
		w	$- 5.5333 \times 10^{-2}$	$- 5.5195 \times 10^{-2}$	$- 5.5380 \times 10^{-2}$	$- 5.5383 \times 10^{-2}$
- 100	0	u	$- 1.2545 \times 10^{-1}$	$- 1.1647 \times 10^{-1}$	$- 1.2567 \times 10^{-1}$	$- 1.2568 \times 10^{-1}$
		w	$- 4.4119 \times 10^{-1}$	$- 4.2375 \times 10^{-1}$	$- 4.4109 \times 10^{-1}$	$- 4.4112 \times 10^{-1}$
- 10	0.3	u	$- 1.8354 \times 10^{-3}$	$- 1.0139 \times 10^{-3}$	$- 1.8420 \times 10^{-3}$	$- 1.8423 \times 10^{-3}$
		w	$- 5.5334 \times 10^{-2}$	$- 4.1082 \times 10^{-2}$	$- 5.5380 \times 10^{-2}$	$- 5.5384 \times 10^{-2}$
- 100	0.3	u	$- 1.2545 \times 10^{-1}$	$- 7.6532 \times 10^{-2}$	$- 1.2567 \times 10^{-1}$	$- 1.2568 \times 10^{-1}$
		w	$- 4.4119 \times 10^{-1}$	$- 3.4829 \times 10^{-1}$	$- 4.4109 \times 10^{-1}$	$- 4.4113 \times 10^{-1}$

Table 4 Displacements of point A when the cantilever beam is in three-dimensional bending state

λ	Direction	Displacement (m)			
		ABAQUS	ANCF-full	ANCF- deficient	GEF
0	u	$- 7.4206 \times 10^{-2}$	$- 7.0279 \times 10^{-2}$	$- 7.4186 \times 10^{-2}$	$- 7.4196 \times 10^{-2}$
	v	$- 2.4337 \times 10^{-1}$	$- 2.3637 \times 10^{-1}$	$- 2.4335 \times 10^{-1}$	2.4337×10^{-1}
	w	$- 2.4337 \times 10^{-1}$	$- 2.3637 \times 10^{-1}$	$- 2.4335 \times 10^{-1}$	$- 2.4337 \times 10^{-1}$
0.3	u	$- 7.4207 \times 10^{-2}$	$- 4.3395 \times 10^{-2}$	$- 7.4186 \times 10^{-2}$	$- 7.4198 \times 10^{-2}$
	v	$- 2.4337 \times 10^{-1}$	$- 1.8746 \times 10^{-1}$	$- 2.4335 \times 10^{-1}$	$- 2.4337 \times 10^{-1}$
	w	$- 2.4337 \times 10^{-1}$	$- 1.8746 \times 10^{-1}$	$- 2.4335 \times 10^{-1}$	$- 2.4337 \times 10^{-1}$

Table 5 Angles of rotation of the free end when the cantilever beam is in pure bending state

Element number	Angles of rotation (°)			
	ANCF-full ($\lambda=0$)	ANCF-full ($\lambda=0.3$)	ANCF-deficient	GEF
10	226.95987	196.59371	360.02526	357.65866
20	334.81350	258.00076	360.22077	359.97302
30	354.55729	265.55132	360.22002	359.97382

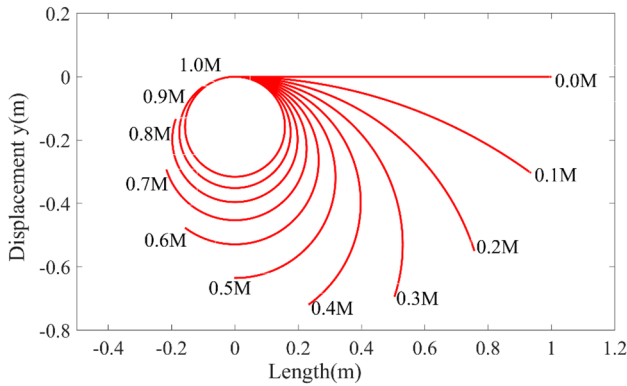


Fig. 5 Diagram of nonlinear large deflection curves with different external moment

element of both ANCF gradient-deficient beam element and GEF beam element are 20. The results of both the ANCF gradient-deficient beam element and the GEF beam element are closer to the exact result of 360° than that of ANCF fully parameterized beam element. While for the ANCF fully parameterized beam element with different Poisson’s ratio, the element number larger than 30 is required to achieve convergence. As a result, the GEF beam element has the high calculation accuracy and efficiency. The diagram of nonlinear large deflection curves calculated by the GEF beam element is shown in Fig. 5, from which the configuration of the beam caused by different various moment can be found intuitively.

For the torsion deformation of the cantilever beam, the torque T is applied to the free end around x -axis. Due to the neglect of the cross section, the ANCF gradient-deficient beam element is not considered to solve the response in this case. The beam has also been divided into 10, 20 and 30

elements, the results based on other two types of elements are given in Table 6 under the conditions of $T = -10$ Nm and $T = -100$ Nm. Table 6 shows that there are good agreements between the results of the GEF beam element and ABAQUS, and the results converge faster when the beam is only discretized into ten elements for GEF beam element. In comparison, the results of the ANCF fully parameterized beam element are quite different from the exact solutions whether Poisson’s ratio exists or not.

According to the above analyses, the suitable element can be selected to solve the static response of the flexible multi-body system with large deformation. The GEF beam element has the highest accuracy among the three beam elements when the beam is in axial tension, axial compression and torsion states. Both the ANCF gradient-deficient beam and the GEF beam element have the higher accuracy and efficiency than that of the ANCF fully parameterized beam element when the beam is bent. It is necessary to note that the GEF beam element is the best choice as the cross-sectional deformation of beam needs to be considered.

Dynamic Response of the Beam Element

To study the accuracy of beam element in dynamics, both the three-dimensional simple and double pendulum models are investigated. Due to the ignorance of the cross-sectional deformation, the ANCF gradient-deficient beam element cannot be adopted to solve the three-dimensional dynamic response. In addition, since commercial software cannot directly simulate the dynamics of the flexible multi-body system with large deformation, the simulation of commercial software is not be adopted in the model. Therefore, only the results of the ANCF fully parameterized beam element and the GEF beam element are analyzed in this section, and the

Table 6 Angles of rotation of the free end when the cantilever beam is in torsion state

T (Nm)	Element number	Angles of rotation (°)			
		ABAQUS	ANCF-full ($\lambda=0$)	ANCF-full ($\lambda=0.3$)	GEF
10	10	14.6740	10.1536	6.3462	14.6739
	20	14.6739	11.2874	7.6534	14.6739
	30	14.6739	13.1453	8.1678	14.6739
100	10	213.061	198.211	164.586	213.261
	20	213.211	205.332	168.427	213.261
	30	213.239	209.432	176.567	213.261

dynamic responses simulated by the GEF beam element with time step of 10^{-4} s are used as reference values.

The Simple Pendulum Model

The dynamic response of the simple pendulum is discussed first. The simple pendulum has a dimension of $1\text{ m} \times 0.01\text{ m} \times 0.01\text{ m}$ as shown in Fig. 6, in which an ideal spherical hinge is used to constrain the fixed end. The density, Poisson’s ratio and Young’s modulus are 2700 kg/m^3 , 0.3 and $3 \times 10^7\text{ Pa}$, respectively, and the flexible body is divided into ten elements in calculation. Applying the initial condition of $\theta = 90^\circ$ and releasing it, the dynamic behaviors of the simple pendulum are induced by gravity.

The displacements of point B which is the geometric center of the free end section along x , y and z direction are shown in Fig. 7a. The results based on the ANCF fully parameterized beam element with time step of 10^{-2} s and

10^{-4} s are denoted by the red solid line and blue long dotted line, respectively. The results obtained by the GEF beam element with time step of 10^{-2} s and 10^{-4} s are represented by the blue short dotted line and the red dotted line, respectively. Figure 7a1 shows that there is a small difference between the displacement along x direction of the ANCF fully parameterized beam element and the GEF beam element, while the varying tendency has a good consistency. In Fig. 7a2, the displacements along y direction of both elements are zero, which means that the dynamic behavior occurs only in x – z plane. In Fig. 7a3, two apparent features can be found, one is that four curves have good consistency at the initial stage and the difference occurs after about 1.5 s, the peaks of the GEF beam element are higher than that of the ANCF fully parameterized beam element at the later stage. It is the effect of the deviation accumulates with time that leads to the gradual increase in the difference. The other feature is that the different time step has an effect on the calculation accuracy. The smaller time step allows a higher iteration accuracy and calculation accuracy during computation, but the simulation time will be longer.

Subsequently, the Young’s modulus of the simple pendulum is transformed into $7 \times 10^{11}\text{ Pa}$ from $3 \times 10^7\text{ Pa}$ to enhance the stiffness of simple pendulum and other calculation conditions remain unchanged. The displacements are shown in Fig. 7b, in which the line types of the curve are the same meaning with the above description. We can find that there is a good agreement among the four curves along x , y , z direction, even though the time steps are different,

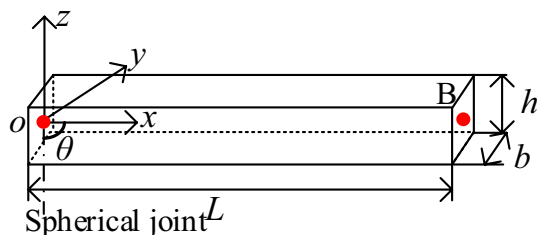


Fig. 6 The schematic of the simple pendulum

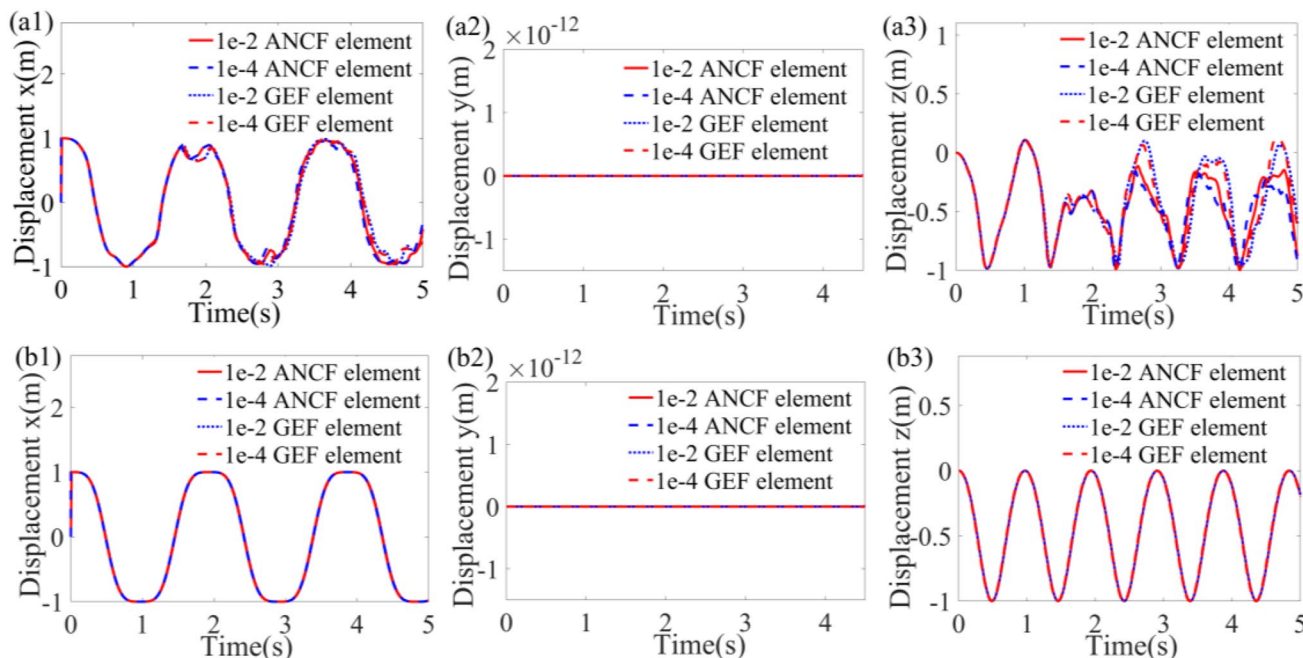


Fig. 7 Displacements of point B along x , y , z direction. The Young’s moduli are (a1–a3) $3 \times 10^7\text{ Pa}$ and (b1–b3) $7 \times 10^{11}\text{ Pa}$, respectively

because the influence of nonlinear factor is weakened by the enhanced stiffness.

The Double Pendulum Model

To further study the accuracy of the ANCF fully parameterized beam element and the GEF beam element used in three-dimensional model, the displacement responses of the double pendulum are analyzed, the corresponding schematic diagram is shown in Fig. 8, in which two flexible rods are connected by a ball joint. At the initial moment, both rods are kept in the horizontal plane, i.e., x - y plane and released, the dynamic behaviors are caused by gravity. Two kinds of Young's modulus are used for calculation and both flexible rods are divided into ten elements, respectively, the time step of 10^{-4} s is adopted, other material and geometric

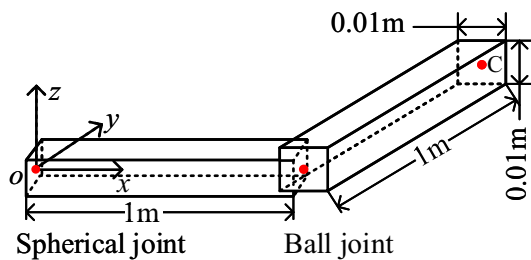


Fig. 8 Schematic diagram of the double pendulum

parameters of the rod are the same as those of the accuracy simple pendulum.

The displacements of point C which is the geometric center of the section along x , y , z direction based on the two beam elements are shown in Fig. 9, in which the Young's modulus of 2×10^8 Pa and 7.2×10^{10} Pa for both rods are applied, respectively. The simulation results of the ANCF fully parameterized beam element and the GEF beam element are denoted by the red solid line and blue dotted line, respectively. Figure 9a shows that the two curves are different at the later stage when Young's modulus is small, while the consistency becomes better with the increase of Young's modulus as shown in Fig. 9b. Such phenomenon is similar with the situation of the simple pendulum, which is also caused by decreasing elastic deformation of the flexible body and the weakened the nonlinear factor.

As a result, it can be concluded that the ANCF fully parameterized beam element and the GEF beam element have higher accuracy for solving dynamic system with large stiffness, while the GEF beam element is the best choice when the stiffness is small.

Conclusions

To achieve the required high accuracy and efficiency in different projects of flexible multibody system with nonlinear large deformation, the characteristics and applicable

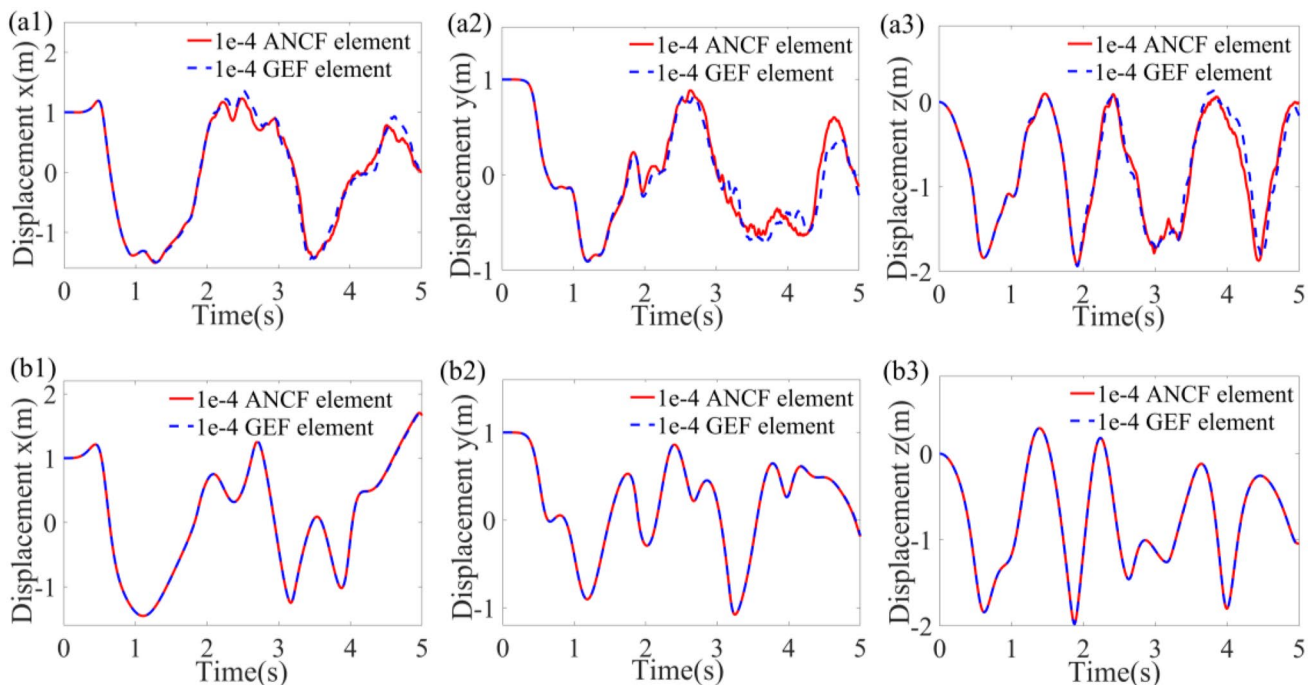


Fig. 9 Displacements of point C along x , y , z direction. The Young's moduli of both rods are (a1–a3) 2×10^8 Pa and (b1–b3) 7.2×10^{10} Pa, respectively

conditions of the commonly used beam elements which are ANCF fully parameterized beam element, ANCF gradient-deficient beam element and GEF beam element are provided by analyzing both static and dynamic models.

In the statics of the flexible multibody system with nonlinear deformation, the displacement responses of the cantilever beam under axial deformation, torsion and bending are analyzed in detail. The GEF beam element is recommended first when the discretized element is subjected to axial tension, axial compression and torsion. When the element is bent, both ANCF gradient-deficient beam and GEF beam element have the high accuracy and efficiency. In addition, the GEF beam element is the unique choice when the deformation of element section is considered.

For dynamics, the cases of both the simple and double pendulums are analyzed. It can be found that the Young's modulus and time step in calculation have a great effect on the displacement response due to the factor of nonlinear deformation. The results of the ANCF fully parameterized beam element and the GEF beam element have good consistency when the Young's modulus is large. While the GEF beam element is the best choice for the small Young's modulus. All the results are helpful for the selection of beam elements to achieve high accuracy and efficiency of multibody system with nonlinear large deformation.

Funding This work is supported in part by the National Natural Science Foundation of China (Grant No. 12102041; 52130512) and China Postdoctoral Science Foundation (Grant No. 2021M690401) and Graduate Technological Innovation Project of Beijing Institute of Technology (Project No. 2019CX10005).

Declarations

Conflict of interest The authors declare no conflict of interest.

References

- Xu JG, Jia JG (2001) Study on dynamics, stability and control of multi-body flexible structure system in functional space. *Appl Math Mech (English Edition)* 22:1410–1421
- Yong A, Huang ZC, Deng LX (2007) Dynamic analysis of a rotating rigid-flexible coupled smart structure with large deformations. *Appl Math Mech (English Edition)* 28:1349
- Hu ZD, Hong JZ (1999) Modeling and analysis of a coupled rigid-flexible system. *Appl Math Mech (English Edition)* 20(10):1167–1174
- Liu ZF, Yan SJ, Fu Z (2013) Dynamic analysis on generalized linear elastic body subjected to large scale rigid rotations. *Appl Math Mech (English Edition)* 34:1001–1016
- Shabana AA (1996) An absolute nodal coordinates formulation for the large rotation and deformation analysis of flexible bodies. University of Illinois at Chicago, Chicago
- Shabana AA (1997) Flexible multibody dynamics review of past and recent development. *Multibody SysDyn* 1:189–222
- Schienen W (2007) Research trends in multibody system dynamics. *Multibody SysDyn* 18:3–13
- Escalona JL, Hussien HA, Shabana AA (1998) Application of the absolute nodal coordinate formulation to multibody system dynamic. *J Sound Vib* 214:833–951
- Shabana AA, Yakoub RY (2001) Three-dimensional absolute nodal coordinate formulation for beam elements: theory. *J Mech Design* 123:606–613
- Yakoub RY, Shabana AA (2001) Three-dimensional absolute nodal coordinate formulation for beam elements implementation and applications. *J Mech Design* 123:614–621
- Berzeri M, Campanelli M, Shabana AA (2001) Definition of the elastic forces in the finite-element absolute nodal coordinate formulation and the floating frame of reference formulation. *Multibody SysDyn* 5:21–55
- Gerstmayr J, Shabana AA (2006) Analysis of thin beams and cables using the absolute nodal coordinate formulation. *Nonlinear Dyn* 45:109–130
- Schwarze M, Reese S (2010) A reduced integration solid shell finite element based on the EAS and the ANS concept-Large deformation problems. *Int J Numer Meth Eng* 85:289–329
- Wu J, Zhao ZH, Ren GX (2012) Dynamic analysis of space structure deployment with transient thermal load. *Adv Mater Res* 479:803–807
- Sopanen JT, Mikkola AM (2003) Description of elastic forces in absolute nodal coordinate formulation. *Nonlinear Dyn* 34:53–74
- Omar MA, Shabana AA, Mikkola A (2004) Multibody system modeling of leaf springs. *J Vib Control* 10:1601–1638
- Liu JY, Lu H (2007) Rigid-flexible coupling dynamics of a flexible beam with three-dimensional large overall motion. *Multibody SysDyn* 18:487–510
- Liu J, Hong J, Cui L (2007) An exact nonlinear hybrid-coordinate formulation for flexible multibody systems. *Acta Mech Sin* 23:699–706
- Liu JY, Lu H (2007) Rigid-flexible coupling dynamics of three-dimensional hub-beams system. *Multibody SysDyn* 18:487–510
- Tian Q, Zhang YQ, Chen LP, Yang JZ (2010) Simulation of planar flexible multibody systems with clearance and lubricated revolute joints. *Nonlinear Dyn* 60:489–511
- Tian Q, Zhang YQ, Chen LP (2009) Dynamics of spatial flexible multibody systems with clearance and lubricated spherical joints. *Comput Struct* 87:913–929
- Tian Q, Chen LP, Zhang YQ (2009) An efficient hybrid method for multibody dynamics simulation based on absolute nodal coordinate formulation. *J Comput Nonlinear Dyn* 4:0210091
- Liu C, Tian Q, Hu HY (2011) Dynamics of a large-scale rigid-flexible multibody system composed of composite laminated plates. *Multibody SysDyn* 26:283–305
- Reissner E (1972) On one-dimensional finite-strain beam theory: the plane problem. *Zeitschrift F Fur Angewandte Mathematik Und Physik* 23:795–804
- Simo JC, Vu-Quoc L (1988) On the Dynamics in space of rods undergoing large motions—a geometrically exact approach. *Comput Methods Appl Mech Eng* 66:125–161
- Crisfield MA, Jelenic G (1999) Objectivity of strain measures in the geometrically exact three-dimensional beam theory and its finite-element implementation [J]. *Proc Royal Soc Math Phys Eng Sci* 455:1125–1147
- Huang G, Zhong P, Yang G (2016) Frame-invariance in finite element formulations of geometrically exact rods. *Appl Math Mech (English Edition)* 37:12
- Romero I (2008) A comparison of finite elements for nonlinear beams: the absolute nodal coordinate and geometrically exact formulations. *Multibody SysDyn* 20:51–68

29. Bauchau OA, Han S, Mikkola A (2014) Comparison of the absolute nodal coordinate and geometrically exact formulations for beams. *Multibody SysDyn* 32:67–85
30. Liu C (2013) Deployment dynamics of flexible space structures described by Absolute-Coordinate-Based Method [D]. Beijing Institute of Technology
31. Bonet J, Wood RD (2008) *Nonlinear continuum mechanics for finite element analysis*, 2nd edn. Cambridge University Press, New York
32. Jelenc G, Crisfield MA (1998) Interpolation of rotational variables in nonlinear dynamics of 3D beams. *Int J Numer Meth Eng* 43:1193–1222
33. Shabana AA (2005) *Dynamics of multibody systems*. Cambridge University Press, New York
34. Shabana A (2010) *Computational dynamics*, 3rd edn. Wiley, New York
35. Arnold M, Brüls O (2007) Convergence of the generalized- α scheme for constrained mechanical systems. *Multibody SysDyn* 18:185–202
36. Tian Q, Liu C, Machado M, Flores P (2011) A new model for dry and lubricated cylindrical joints with clearance in spatial flexible multibody systems. *Nonlinear Dyn* 64:25–67
37. Liu C, Tian Q, Hu H (2012) Dynamics and control of a spatial rigid–flexible multibody system with multiple cylindrical clearance joints. *Mech Mach Theory* 52:106–129
38. Timoshenko S, Gere J (1972) *Mechanics of materials*. Van Nostrand Reinhold Co., New York

Publisher's Note Springer Nature remains neutral with regard to jurisdictional claims in published maps and institutional affiliations.